CONF-830301--7

SAND--82-0899C

DE83 005191

SAND82-0899

A QUASI-STEADY MODEL FOR PREDICTING TEMPERATURE OF AQUEOUS FOAMS CIRCULATING IN GEOTHERMAL WELLBORES

Bennie F. Blackwell
Thermal Test and Analysis, Div. 7537

Alfonso Ortega
Fluid Mechanics and Heat Transfer Division II, Div. 1512

Sandia National Laboratories
Albuquerque, New Mexico 87185

ABSTRACT

A quasi-steady model has been developed for predicting the temperature profiles of aqueous foams circulating in geothermal wellbores. The model assumes steady one-dimensional incompressible flow in the wellbore; heat transfer by conduction from the geologic formation to the foam is one-dimensional radially and time-dependent. The vertical temperature distribution in the undisturbed geologic formation is assumed to be composed of two linear segments. For constant values of the convective heat-transfer coefficient, a closed-form analytical solution is obtained. It is demonstrated that the Prandtl number of aqueous foams is large (1000 to 5000); hence, a fully developed temperature profile may not exist for representative drilling applications. Existing convective heat-transfer-coefficient solutions are adapted to aqueous foams. The simplified quasi-steady model is successfully compared with a more-sophisticated finite-difference computer code. Sample temperature-profile calculations are presented for representative values of the primary parameters. For a 5000-ft wellbore with a bottom hole temperature of 375°F, the maximum foam temperature can be as high as 300°F.

DISCLAIMER

Nomenclature

A	heat-transfer area, $A_i = \pi d_i L$
$B_1, B_2, C_1, C_2,$ $D_1, D_2, E_1, E_2,$	constants in solution of energy equation, Eq. (A-13)
Bi	Biot number for formation; see Eq. (B-4)
C_p	specific heat at constant pressure of foam
C_{p_g}, C_{p_ℓ}	specific heat at constant pressure of gas and liquid components of foam
d	pipe diameter; see Figure 1 for specific definition of d_i, i=1,2,---,5
f	integral heat loss function tabulated by Willhite [23]; see discussion of Eq. (B-7).
Fo	Fourier number for formation; see Eq. (B-4)
g	acceleration of gravity, 32.174 ft/s^2=980.7 cm/s^2
g_c	Newton constant, 32.174 ft-lbm/(lbf-s^2)=1 m-kg/(N-s^2)
G	dimensionless heat loss function, see Eq. (B-6)
h	convective heat-transfer coefficient
h_i	i=1,2,3 convective heat transfer coefficient for surface i
$\bar{h}_i$	i=1,2,3 convective heat-transfer coefficient averaged over length L_e.
H	constant defined by Eq. (A-14)
i	enthalpy of foam
I_J	integral heat loss function tabulated by Jessop [28]; see discussion of Eq. (B-8),
J	mechanical equivalent of heat 777.66 ft-lbf/Btu = 1 N-m/J
k, k_g, k_ℓ	thermal conductivity of foam, gas and liquid components of foam, respectively

L	wellbore length
L_e	length over which the convective heat-transfer coefficient is averaged
L^*	depth at which the bilinear geothermal temperature profiles are joined; see Figure A-1
$\dot{m}$	mass flow rate of foam
Nu	Nusselt number for various wellbore geometries, $Nu = hd/k$ or $h\delta/k$
N_{tu}	number of transfer units, $N_{tu_i} = U_i A_i/(\dot{m}C_p)$
P	perimeter, $P_i = \pi d_i$; also, constant in Eq. (A-14)
Pe	Peclet number of foam, $Pe = \bar{V}d/\alpha$
Pr	Prandtl number of foam, $Pr = C_p\mu/k$
q_1, q_3	heat flow per unit area A_1, A_3
Re	Reynolds number of foam, $Re = \rho d\bar{V}/\mu$
t	time
T	temperature
T_c, T_h	temperature of "cold" and "hot" fluids, respectively
T_{c_i}	inlet temperature of foam at surface
T_o, T_2	formation temperatures, see Figure A-1
$T_\infty(z)$	undisturbed geothermal temperature as a function of depth
U_1, U_3	overall heat-transfer coefficient based on area A_1 or A_3; see Eqs. (B-1) and (B-3)
U_3^o	value of U_3 at time zero, see Eq. (B-2)
$\bar{V}$	foam velocity, averaged over pipe cross section
y_ℓ	mass fraction of liquid component in foam
x	dummy integration variable
z	depth below surface

α_e	thermal diffusivity of earth
β	gravitational parameter, $\beta = gL/(g_c JC_p \Delta T)$
γ	geothermal gradient of linear profile
γ_i	i=1,2 geothermal gradient over Regions 1 or 2 of bilinear profile
δ	annulus gap spacing; see Eq. (16)
ΔT	formation temperature difference between bottom of hole and surface; see Eq. (A-7) and Figure A-1
ζ	dimensionless depth, $\zeta = z/L$
ζ^*	$= L^*/L$
θ	dimensionless temperature, $\theta = (T-T_{c_i})/\Delta T$
θ_∞	$= [T_\infty(z)-T_c]/\Delta T$
λ_1, λ_2	eigenvalues; see Eq. (5)
μ	viscosity
ρ, ρ_ℓ, ρ_g	density of foam and liquid and gas components of foam, respectively
τ	dummy integration variable
ϕ	foam liquid volume fraction

SAND82-0899

A QUASI-STEADY MODEL FOR PREDICTING TEMPERATURE OF AQUEOUS FOAMS CIRCULATING IN GEOTHERMAL WELLBORES

Introduction

Aqueous foams have many applications ranging from fire fighting to petroleum drilling. References 1-13 discuss the hydrodynamic characteristics of these foams, primarily from the standpoint of use as drilling fluids. Some of the reported advantages of foams as drilling fluids are:

- Their low density means low pressures at the bottom of a hole.
- Sand and cuttings fall back very little when circulation stops.
- There is low loss of circulation.

These reported advantages of foams for drilling in petroleum formations are also advantages for drilling in geothermal applications. However, it is not known if drilling foams can function in geothermal environments with temperatures approaching 250°C (482°F). To investigate the stability of aqueous foams at elevated temperatures, an estimate of the maximum temperature the foam reaches in a given wellbore configuration is important. In response to this need, we developed a simple analytical model for estimating temperature of aqueous foams circulating in a geothermal wellbore. This paper describes our quasi-steady heat-transfer model for drilling foams and presents some results from parameter studies. Detailed development of the mathematical model is presented in Appendices A and B.

Description of Quasi-Steady Temperature Model

Figure 1 is a schematic of a simplified wellbore. Drilling foam generated at the surface is injected into the drill pipe; the foam then flows down the drill pipe and back up the annulus. Heat is transferred from the hot formation to the annulus fluid, which in turn loses some of its heat to the fluid flowing down the drill pipe. All heat-transfer rates are assumed proportional to a temperature-difference driving potential, with the proportionality constant being the overall heat-transfer coefficient U. The fluid flowing down the drill pipe is called the "cold" fluid; that in the annulus is called the "hot" fluid. If steady one-dimensional flow of an incompressible fluid is assumed, the energy equation for the "cold" and "hot" fluids can be written as

$$\dot{m}\frac{d}{dz}\left(i_c + \frac{\bar{V}_c^2}{2g_c J} - \frac{g}{g_c}\frac{z}{J}\right) - U_1 P_1 (T_h - T_c) = 0 \qquad (1)$$

$$-\dot{m}\frac{d}{dz}\left(i_h + \frac{\bar{V}_h^2}{2g_c J} - \frac{g}{g_c}\frac{z}{J}\right) + U_1 P_1 (T_h - T_c) - U_3 P_3 [T_\infty(z) - T_h] = 0 \qquad (2)$$

where P is the perimeter of the appropriate pipe section through which heat is being transferred and $T_\infty(z)$ is the temperature of the undisturbed geologic formation at a radial distance far removed from the wellbore. We will assume that kinetic energy is small in comparison to potential energy and enthalpy.

Contrary to the assumption stated above, drilling foam is compressible; however, compressibility effects will have a relatively minor impact on the predicted temperature profile. In the energy equations given above, compressibility influences the terms of kinetic energy per unit mass ($\bar{V}^2/2$) and the determination of the overall heat-transfer coefficients (U_1, U_3). It can be demonstrated that terms for internal and potential energy are somewhat larger than terms for kinetic energy; hence, compressibility has little impact on the energy content of the foam. As shown later, the overall heat-transfer coefficients U_1

and U_3 depend on individual convective heat-transfer coefficients that in turn depend on ρ and $\bar{V}$. Fortunately, the convective heat-transfer coefficients generally depend on the "mass-velocity" $\rho\bar{V}$, which remains constant under steady flow conditions with constant flow area. Since the assumption will be made that U_1 and U_3 are independent of wellbore position, and that $\rho\bar{V}(=\dot{m}/A)$ is also independent of position by means of the continuity equation, incompressible flow does not seem unreasonable. One of the primary motivating factors for assuming U_1 and U_3 are independent of position is that this assumption allows us to obtain closed-form analytical solutions, which in turn gives some insight into the parameters governing the temperature profile. If predicting pressure variation along with temperature variation in the wellbore is of interest, then compressibility effects become more significant.

For the case of a linear vertical geothermal profile and enthalpy replaced by heat capacity times temperature, the solution to Eqs. (1) and (2) can be written as

$$\theta_c = \frac{T_c - T_{c_i}}{\Delta T} = \frac{T_o - T_{c_i}}{\Delta T} + \frac{1}{N_{tu_1}}(\beta - 1) + \zeta + D_1 e^{\lambda_1 \zeta} + E_1 e^{\lambda_2 \zeta} \tag{3}$$

$$\theta_h = \frac{T_h - T_{c_i}}{\Delta T} = \frac{T_o - T_{c_i}}{\Delta T} + \zeta + \left(1 + \frac{\lambda_1}{N_{tu_1}}\right) D_1 e^{\lambda_1 \zeta} + \left(1 + \frac{\lambda_2}{N_{tu_1}}\right) E_1 e^{\lambda_2 \zeta} \tag{4}$$

where $\beta = \dfrac{gL}{g_c J C_p \Delta T}$, $\Delta T = \gamma L$, $\zeta = z/L$, $N_{tu_i} = \dfrac{(UA)_i}{\dot{m} C_p}$

$$\lambda_1 = \frac{N_{tu_3}}{2}\left(1 + \sqrt{1 + 4\,\frac{N_{tu_1}}{N_{tu_3}}}\right)$$

$$\lambda_2 = \frac{N_{tu_3}}{2}\left(1 - \sqrt{1 + 4\,\frac{N_{tu_1}}{N_{tu_3}}}\right) \tag{5}$$

$$E_1 = \frac{\lambda_1 e^{\lambda_1}\left[\dfrac{T_o - T_{c_i}}{\Delta T} + \dfrac{1}{N_{tu_1}}(\beta - 1)\right] + \beta - 1}{\lambda_2 e^{\lambda_2} - \lambda_1 e^{\lambda_1}}$$

$$D_1 = -\left[E_1 + \frac{T_o - T_{c_i}}{\Delta T} + \frac{1}{N_{tu_1}}(\beta - 1)\right]$$

Additional details on the above solution are furnished in Appendix A where the solution is developed for a bilinear geothermal profile. From Eqs. (3)-(5), the dimensionless temperature profile depends on the following four parameters:

$$\beta = \frac{gL}{g_c J C_p \Delta T} : \quad \text{gravitational}$$

$$\frac{T_o - T_{c_i}}{\Delta T} : \quad \text{formation to cold-fluid temperature difference at surface}$$

$$N_{tu_1} = \frac{U_1 A_1}{\dot{m} C_p} :$$

$$N_{tu_3} = \frac{U_3 A_3}{\dot{m} C_p} : \quad \Bigg\} \text{ number of transfer units}$$

The specification of these four parameters completely determines the dimensionless temperature profile. Typical results are shown in Figure 2 for several values of (N_{tu_1}, N_{tu_3}) along with representative values for ($T_o - T_{c_i}$) and β. Because the temperature is normalized by the temperature difference between the bottom of the hole and the surface of the undisturbed geologic formation, the maximum value of θ is unity. Several general conclusions can be drawn from the results in Figure 2.

(1) The maximum temperature of the fluid always occurs in the annulus, where both the magnitude of the maximum temperature and the depth at which it occurs are strong functions of N_{tu_1} and N_{tu_3}. Increasing N_{tu_1} and/or N_{tu_3} increases both the maximum temperature and its corresponding depth.

(2) The temperature of the "hot" fluid can be either above or below that of the local undisturbed geologic formation. It is physically realistic for the "hot" fluid temperature to exceed the undisturbed geothermal temperature because, in the direction of "hot" fluid flow, the geothermal temperature decreases at a faster rate than that temperature of the drilling fluid.

(3) The return temperature of the "hot" fluid increases for decreasing values of $N_{tu_1}(N_{tu_3})$ while keeping $N_{tu_3}(N_{tu_1})$ constant. The return temperature is not so sensitive to changes in (N_{tu_1}, N_{tu_3}) as was the maximum temperature. Measurement of the "hot" fluid return temperature will thus yield little information about the maximum temperature experienced by the foam.

(4) Changing N_{tu_3} while keeping N_{tu_1} fixed has a greater effect on the temperature profile of the "hot" fluid than on that of the "cold" fluid.

(5) In the limit as (N_{tu_1}, N_{tu_3}) approach infinity, the temperature profile of the drilling fluid approaches that of the undisturbed geothermal profile.

The results of Figure 2 were constructed by using arbitrary values of (N_{tu_1}, N_{tu_3}). In reality, both N_{tu_1} and N_{tu_3} are determined by the wellbore and heat-transfer characteristics of the drilling fluid with N_{tu_3} also a function of time. Procedures for calculating the overall heat-transfer coefficient are discussed in Appendix B; calculation of the average heat-transfer coefficient for drilling foams is discussed in the next section.

Calculation of Average Heat-Transfer Coefficient for Aqueous Forms

Techniques for calculating the overall heat-transfer coefficient for wellbore configurations are discussed in Appendix B. One of the necessary parameters is the convective heat-transfer coefficient between the flowing foam and the pipe walls. This section presents a model for the convective heat-transfer coefficient of aqueous foams flowing in pipe and annulus geometries.

An understanding of some of the characteristics of the convective heat-transfer behavior of aqueous forms is needed before this behavior can be modeled. Aqueous foams are mixtures of a gas and liquid (surfactant) in which the liquid phase is the continuous phase. Bikerman [14] describes foams as agglomerations of gas bubbles separated from each other by thin liquid films, as opposed to gas emulsions in which the thickness of the interstitial liquid layers is of the same order as the diameter of the bubble. The relative consistency of an aqueous foam may be described by the size distribution of the bubbles and the liquid volume fraction ϕ of the foam.

$$\phi = \frac{\text{Liquid Volume}}{\text{Liquid Volume + Gas Volume}}$$

One of the desirable characteristics of aqueous foams is their high apparent viscosity, which allows cuttings to be removed with relatively low annulus velocities. It has been shown by Beyer [3] that for a given velocity, the drag on a 3/16-in-dia sphere with foam flow is a maximum at a liquid volume fraction of about 0.04, decreasing to a relative minimum at about 0.3. This coincides qualitatively with the expected variation of apparent viscosity with ϕ, and as a general rule the foam should be circulated within these limits for efficient chip removal at nominal flow rates.

The most comprehensive investigation of foam circulation in wellbores is probably that of Beyer, Millhone, and Foote [3]. They assumed that foam could be treated as a Bingham plastic [15]. The apparent viscosity was obtained from pilot-scale experiments and was correlated as a function of liquid volume fraction. Although the viscosity probably depends on liquid volume fraction (ϕ) and other parameters, the results of [15] represent the most complete data available and are used for this study. Their results are as follows.

$$\mu = \frac{1}{7200\phi+267} \text{ [lbf-sec/ft}^2\text{]}, \quad 0.02 \leq \phi \leq 0.10$$

$$\mu = \frac{1}{2533\phi+733} \text{ [lbf-sec/ft}^2\text{]}, \quad 0.1 < \phi \leq 0.25 \tag{7}$$

Because all of their experiments were at room temperature, no information is known about the dependence of μ on temperature. Using the empirical viscosity correlation given by Eq. (7) and the momentum equation, Beyer, Millhone, and Foote [3] compared pressure predictions with field test data in two 3000-ft(1000-m) wells.

It is well established that the Prandtl number ($Pr=\mu C_p/k$) influences convective heat-transfer rates. Hence, let us calculate Pr for aqueous foams. Eq. (7) is used for the viscosity μ. If the mass fraction (y) of the liquid and gas components is known, then the heat capacity is a simple function of the component heat capacities.

$$C_p = y_\ell C_{p_\ell} + (1-y_\ell)C_{p_g} \tag{8}$$

Experiments by Drotning, Ortega and Havey [16] indicate that the conductivity of the foam can be approximately related to the component conductivities by the so-called "parallel ordered" model

$$k = \phi k_\ell + (1-\phi)k_g \tag{9}$$

Using Eqs. (7)-(9), we estimated that the foam Prandtl number lay in the range $1000<Pr<5000$. From a heat-transfer point of view, a large value of Pr indicates that the velocity profile in pipe flow

develops much faster than the temperature profile. For a laminar Newtonian fluid, Kays and Crawford [17] indicate that the local friction factor is within 2% of its fully developed value when

$$\frac{Re}{z/d} \leq 20 \text{ or, } \frac{z}{d} \geq \frac{Re}{20} \text{ (velocity profile development)} \quad (10)$$

The calculations of Millhone, Haskin, and Beyer [4] for a petroleum-drilling foam application were used to calculate a representative Reynolds Number; Re seems to be less than about 1000 (based on drill pipe ID). This implies that a laminar Newtonian fluid becomes fully developed in about 50 tube diameters. Although aqueous foams have been reported to have a definite yield strength, the laminar Newtonian model should be an approximate indicator of the distance required for full development of the foam flow.

A similar analysis for the distance required to approach a fully developed temperature profile for a laminar Newtonian fluid is available in Kays and Crawford [17]:

$$\frac{z}{d} \geq \frac{Pe}{20} = \frac{RePr}{20} \quad \text{(temperature profile development)} \quad (11)$$

where Pe is the Peclet number (Vd/α). For a Re of 1000 and Pr of 1000, about 50,000 tube diameters are needed to achieve a fully developed temperature profile. If d_1=2.5 in.(6.35 cm), the development length would be 4167 ft(1283 m). This length indicates that foam applications may exist in which the temperature profile never becomes fully developed. Because of their low thermal diffusivity (high Pr), aqueous foams should be classified as relatively poor heat-transfer mediums.

Problems of thermal entry length for large Pr (or Pe) fluids are often analyzed by assuming that the velocity profile is fully developed while the temperature profile is developing. This assumption allows much simplification in the analysis. For example, Bird, Armstrong, and Hassager [18] present results for the thermally developing Nussult number of an incompressible laminar Newtonian fluid with large Pe and a constant wall-temperature boundary condition.

$$Nu = \frac{hd}{k} = \frac{2}{9^{1/3}\Gamma(4/3)}\left(Pe\ \frac{d}{z}\right)^{1/3} = 1.0768\left(Pe\ \frac{d}{z}\right)^{1/3} \quad (12)$$

Some investigators have reported slip at the wall plus a definite yield strength for foams, calling into question the validity of using Eq. (12) for foams. The extreme case of slip would be a velocity profile that is uniform and equal to the slip velocity, a condition known as plug flow. The plug-flow solution for the case corresponding to Eq. (12) is also given in Bird, Armstrong, and Hassager [18].

$$Nu = \frac{1}{\sqrt{\pi}}\left(Pe\ \frac{d}{z}\right)^{1/2} = 0.5642\left(Pe\ \frac{d}{z}\right)^{1/2} \quad (13)$$

Results of the parabolic and plug flow velocity profile heat transfer are compared in Figure 3. Plug-flow results are always greater than those of laminar Newtonian flow; they represent a reasonable upper limit for the behavior of the heat-transfer coefficient. Similar equations are also presented in Bird, Armstrong, and Hassager [18] for constant heat-flux boundary conditions; only the numerical constant changes for the two different boundary conditions. A model for how the heat-transfer coefficient varies with the flow parameters allows calculation of both the temperature gradient (dT_w/dz) of the pipe wall and the heat flux gradient (dq/dz). Estimates indicate that the gradient of the wall temperature is generally smaller than that of the heat flux. Hence, constant wall temperature seems the more appropriate choice over constant heat-flux boundary conditions for geothermal wellbores.

In the solution of the energy equation given by Eqs. (1)-(2), we assumed that all convective heat-transfer coefficients are independent of position. However, because of the large value of Pe, the convective heat-transfer coefficient certainly is a function of depth. Therefore, Eqs. (12) and (13) need to be averaged over an appropriate length before the quasi-steady model can be applied. If

the average length is denoted by L_e, the average Nusselt No. relationships become

$$\overline{Nu} = \frac{\bar{h}d}{k} = 1.1652 \left(Pe \frac{d}{L_e}\right)^{1/3} \quad \text{Laminar Newtonian} \qquad (14)^*$$

$$\overline{Nu} = \frac{\bar{h}d}{k} = 1.1284 \left(Pe \frac{d}{L_e}\right)^{1/2} \quad \text{Plug Flow} \qquad (15)^*$$

At first glance, it would appear that the effective length L_e should be chosen equal to the wellbore depth L. The presence of tool joints on a nominal spacing of 30 ft suggests consideration of L_e = 30 ft. There are many different types of tool joints (internal upset, external upset, internal-external upset, see Ref [19] for details), but they all have in common a reduction of flow area. This reduction gives rise to a favorable pressure gradient (pressure decreasing in flow direction) and a corresponding flow acceleration. When the flow area is increased back to its original value, the fluid is subjected to an adverse pressure gradient (pressure increasing in flow direction) and can lead to flow separation from the downstream edge of the tool joints. It is well established that laminar flows are much more susceptible to separation than are turbulent flows. The moderately low Reynolds number (Re<1000) for representative foam flows means that separation is very likely to occur from the downstream edge of the tool joint. This separation should cause considerable mixing and possible increases in both pressure drop and the local rate of heat transfer. Heat-transfer rates in developing flows are generally inversely proportional to the thickness of the thermal boundary layer. If a new boundary layer originates after each tool joint, then the local (and average) heat-transfer increases. Calculations are presented for both L_e=30 ft and L_e=L.

*Note that $\bar{h}$ depends on mass velocity $\rho\bar{V}$ (which is constant) instead of ρ and $\bar{V}$ individually.

The hydrodynamic and heat-transfer behavior in the annulus is much more complicated than that in the drill pipe because of pipe/casing eccentricity, the presence of cuttings, drilling in an open hole, and other factors. For the heat-transfer problem, boundary conditions are different for the inner and outer surfaces of the annulus. Since the heat transfer problem for the annulus is not as tractable as that for the pipe, some additional simplifying assumptions are made. The annulus with diameters d_2 and d_3 is replaced by a two-dimensional channel of height equal to

$$\delta = \frac{1}{2}(d_3 - d_2) \tag{16}$$

Bird, Armstrong, and Hassager [18] present solutions for laminar Newtonian and plug flow in this geometry for constant wall-temperature boundary conditions

$$Nu_2 = \frac{h_2\delta}{k} = \left(\frac{3}{4}\right)^{1/3} \frac{2}{9^{1/3}\Gamma(4/3)} \left(\frac{\bar{V}_a\delta}{\alpha}\frac{\delta}{z}\right)^{1/3} \quad \text{Laminar Newtonian} \tag{17}$$

$$Nu_2 = \frac{h_2\delta}{k} = \frac{1}{\sqrt{\pi}}\left(\frac{\bar{V}_a\delta}{\alpha}\frac{\delta}{z}\right)^{1/2} \quad \text{Plug Flow} \tag{18}$$

The plug-flow result for the annulus is identical to that for the pipe if d is replaced by δ; the laminar Newtonian result for the annulus picks up an additional factor of $(3/4)^{1/3}$. Integrating Eqs. (17) and (18) over an effective length L_e, we obtain

$$\overline{Nu}_2 = \frac{\bar{h}_2\delta}{k} = 1.4675\left(\frac{\bar{V}_a\delta}{\alpha}\frac{\delta}{L_e}\right)^{1/3} \quad \text{Laminar Newtonian} \tag{19}$$

$$\overline{Nu}_2 = \frac{\bar{h}_2\delta}{k} = 1.1284\left(\frac{\bar{V}_a\delta}{\alpha}\frac{\delta}{L_e}\right)^{1/2} \quad \text{Plug Flow} \tag{20}$$

It is also assumed that the average convective heat-transfer coefficient on the exterior of the annulus ($\bar{h}_3$) equals that on the interior of the annulus ($\bar{h}_2$).. This assumption should be re-evaluated when foam flows are better understood.

Although there is room for improvement in the proposed convective heat transfer coefficient model, we feel that the plug-flow model is an upper limit and it is unlikely that the heat-transfer rates will be much below those of the laminar Newtonian model. Results from parameter studies comparing plug flow and laminar Newtonian flow are presented in a subsequent section.

Comparison of Quasi-Steady Model With Finite-Difference Model of Wooley [20-22]

Several simplifying assumptions have been made in the development of the quasi-steady model (see Appendix A for details). One of the more significant assumptions was the simple way in which heat is transferred by conduction from the formation to the wellbore. The quasi-steady model decouples the transfer of heat from the formation and from the wellbore; the model of Wooley [20-22] uses a finite-difference procedure to simultaneously solve the energy equations for the formation and wellbore. The Wooley [20-22] model gains accuracy and generality at the expense of computational complexity.

To verify the quasi-steady model, we solved the same problem with both the quasi-steady model and the GEOTEMP* code of Wooley [20-22]. As Figure 4 shows, the comparison is quite good. Circulation time for the comparison is 24 hr. For times earlier than 24 hr, the agreement is not as good because the GEOTEMP code uses the initial temperature profile for both the formation and the wellbore. The quasi-steady model has no way of considering the initial temperature profile of the wellbore fluid. For times greater than 24 hr, the agreement improves. For engineering purposes, the quasi-steady model is adequate for many problems, but it should not be used for problems in which the initial temperature profile of the wellbore is important.

*The incompressible flow version of GEOTEMP was used for all the calculations reported herein.

Sample Calculations for Aqueous Foams

Calculations have been made for a representative geothermal wellbore. The fixed parameters used for the calculations are presented in Table 1. Figure 5 compares various lengths over which the heat-transfer coefficient is averaged, all for the plug-flow heat-transfer model. Curve I is representative of the expected behavior if the tool joints do not enhance heat transfer; for this case, maximum temperature is about 168°F. Curve III is representative of the expected behavior if the tool joints enhance the heat transfer on the surfaces of the inner pipe as well as both sides of the annulus; for this case, maximum temperature is about 306°F. Curve II is an intermediate case where heat transfer for the pipe flow is not enhanced by the tool joints, but the heat transfer of the annulus flow is enhanced. The maximum temperature of the foam is very sensitive to the length over which the heat-transfer coefficient is averaged; the return temperature is much less sensitive. All calculations shown in Figure 5 are for a circulation time of 24 hr. While N_{tu_1} is independent of time, N_{tu_3} is a maximum at time zero and decreases with increasing time. Decreasing N_{tu_3} while keeping all other parameters fixed reduces the maximum foam temperature.

Table 1: Parameters for Figs. 5 and 6

$d_1 = 2.441$ in., $d_2 = 2.875$ in., $d_3 = 6.276$ in., $d_4 = 7.000$ in., $d_5 = 9.625$ in

$k_p = 26.0$ Btu/hr-ft-°F, $k_c = 0.51$ Btu/hr-ft-°F, $k_c = 1.4$ Btu/hr-ft-°F, $\alpha_e = 0.04$ ft^2/hr, $k_g = 0.0206$ Btu/hr-ft-°F, $k_\ell = 0.395$ Btu/hr-ft-°F, $\rho_g = 2.537$ lbm/ft^3, $\rho_\ell = 62.4$ lbm/ft^3, $C_{p_g} = 0.24$ Btu/lbm-°F, $C_{p\ell} = 1.0$ Btu/lbm-°F, $\phi = 0.152$, $\gamma = 0.06$ °F/ft, $\dot{m} = 1.055 \times 10^4$ lbm/hr, $R_{e_1} = 637.3$, $Pe_1 = 7.321 \times 10^5$, $T_o = T_{c_i} = 75$°F.

Circulation time = 24 hr

Figure 6 compares the plug flow and laminar Newtonian flow models for two different averaging lengths. The plug-flow model always gives a larger value for the maximum foam temperature than does the laminar Newtonian flow model because the average heat-transfer coefficient is greater. Curves A and B are representative of the expected behavior if the tool joints do not enhance the heat-transfer coefficient. For large values of averaging length, both the plug and laminar Newtonian flow heat-transfer models yield similar values of average heat-transfer coefficient, as evidenced by the closeness of Curves A and B in Figure 6. Curves C and D are representative of the expected behavior if the tool joints appreciably enhance the local heat-transfer rate; for this condition, the plug and laminar Newtonian flow models are much different. We believe that the plug-flow model is reasonably close to an upper limit on the average heat-transfer coefficient. Unfortunately, the laminar Newtonian flow model does not necessarily represent a lower limit on the average heat transfer but the lower limit will probably not differ greatly from results of the laminar Newtonian flow.

Summary and Conclusions

A quasi-steady model has been developed for the temperature profile of aqueous foams circulating in geothermal wellbores. The foam is assumed to be incompressible allowing an analytical solution of the energy equation after the energy equation has been decoupled from the momentum equation. The term "quasi-steady" comes from assuming that in the energy equation, flow in the wellbore is steady, while conduction heat transfer within the formation is time-dependent. The rate of conduction heat transfer from the formation into the wellbore was computed from an analytical solution for the response of an infinite region bounded internally by a hole and subjected to a convective boundary condition. This approach has been used by many other investigators.

Solutions were presented for linear and bilinear geothermal temperature profiles. The appropriate dimensionless parameters governing the solution have been identified. The most important parameters are the Number of Transfer Units (N_{tu_i}), a term derived from the heat exchanger literature. An increase in either N_{tu_1} or N_{tu_3} while keeping the other fixed increases the maximum temperature of the foam. The quasi-steady model was compared to the more sophisticated finite-difference computer code GEOTEMP, with good agreement obtained for times longer than 24 hr.

Aqueous foams have a very high Prandtl (Pr) number (1000 to 5000). Large Pr fluids require great distances for full development of the temperature profile. Entry length heat-transfer solutions available in the literature were adapted for use with aqueous foams. Both plug-flow and laminar Newtonian flow models were considered. Sample calculations were performed for both plug and laminar flow models with various lengths over which the heat-transfer coefficient was averaged. It was demonstrated analytically that tool joints have the potential for appreciably enhancing the local convective heat-transfer rate. However, the separating flow from the trailing edge of the tool joints is complicated enough that experiments should be run to better quantify the degree of enhancement on the local rate of heat transfer. These experiments are under way at Sandia National Laboratories.

REFERENCES

1. H. G. Wenzel, T. E. Stelson, and M. Brungraber, "Flow of High Expansion Foams in Pipes," ASCE Journal of the Engineering Mechanics Division, pp 153-165, December 1967.

2. A. David and S. S. Marsden, "The Rheology of Foam," SPE Paper No. 2544, Presented at 44th Annual Fall Meeting of SPE, Denver, Colo., Sept. 28-Oct. 1, 1969.

3. A. H. Beyer, R. S. Millhone and R. W. Foote, "Flow Behavior of Foam as a Well Circulating Fluid," SPE Paper No. 3986, presented at 47th Annual Fall Meeting of SPE, San Antonio, Texas, Oct. 8-11, 1972.

4. R. S. Millhone, C. A. Haskin and A. H. Beyer, "Factors Affecting Foam Circulating in Oil Wells," SPE Paper No. 4001, Presented at 47th Annual Fall Meeting of SPE, San Antonio, Texas, Oct. 8-11, 1972.

5. B. J. Mitchell, "Test Data Fill Theory Gap on Using Foam as a Drilling Fluid," The Oil and Gas Journal, Sept. 6, 1971, pp 96-100.

6. G. W. Anderson, "Near-Gauge Holes Through Permafrost," The Oil and Gas Journal, Sept. 20, 1971, pp. 128-142.

7. J. A. Krug and B. J. Mitchell, "Charts Help Find Volume, Pressure Needed for Foam Drilling," The Oil and Gas Journal, February 7, 1972, pp 61-64.

8. R. E. Blauer, B. J. Mitchell and C. A. Kohlhaas, "Determination of Laminar, Turbulent, and Transitional Foam-Flow Friction Losses in Pipes," SPE Paper No. 4885, Presented at 44th Annual California Regional Meeting, San Francisco, CA, April 4-5, 1974.

9. R. E. Blauer and C. A. Kohlhaas, "Formation Fracturing with Foam," SPE Paper No. 5003, presented at SPE 49th Annual Fall Meeting, Houston, TX, Oct. 6-9, 1974.

10. R. L. Essary and E. E. Rogers, "Techniques and Results of Foam Redrilling Operations - San Joaquin Valley, California," SPE Paper No. 5715, Presented at SPE Symposium on Formation Damage Control, Houston, TX, Jan. 29-30, 1976.

11. N. W. Bentsen and J. N. Veny, "Preformed Stable Foam Performance in Drilling Evaluating Shallow Gas Wells in Northeastern Alberta," SPE Paper No. 5712, Presented at SPE Symposium on Damage Control", Houston, TX, Jan. 29-30, 1976.

References (cont)

12. D. L. Lord, "Analysis of Dynamic and Static Foam Behavior," JPT, Jan. 1981, pp. 39-45.

13. D. L. Holcomb, E. Callaway and L. L. Curry, "Chemistry, Physical Nature, and Rheology of Aqueous Stimulation Foams," SPE Journal, Aug. 1981, pp. 410-414.

14. J. J. Bikerman, Foams, Springer-Verlag, New York, 1973, p. 1.

15. R. B. Bird, W. E. Stewart and E. N. Lightfoot, Transport Phenomena, John Wiley and Sons, New York, 1969.

16. W. D. Drotning, A. Ortega and P. E. Havey, "Thermal Conductivity of Aqueous Foam," SAND82-0742, May, 1982.

17. W. M. Kays and M. E. Crawford, Convective Heat and Mass Transfer, McGraw-Hill, New York, 1980.

18. R. B. Bird, R. C. Armstrong and O. Hassager, Dynamics of Polymeric Liquids-Fluid Mechanics, Vol. I, John Wiley, New York, 1977.

19. "API Specification for Casing, Tubing, and Drill Pipe," American Petroleum Institute, API Spec 5A, March, 1979.

20. G. R. Wooley, "Wellbore and Soil Thermal Simulation for Geothermal Wells: Development of Computer Model and Acquisition of Field Temperature Data," Sandia Laboratories, SAND79-7119, March, 1980.

21. G. R. Wooley, "Wellbore and Soil Thermal Simulation for Geothermal Wells: Comparison of Geotemp Predictions to Field Data and Evaluation of Flow Variables," Sandia Laboratories, SAND79-7116, March, 1980.

22. G. R. Wooley, "Computing Downhole Temperatures in Circulation, Injection, and Production Wells," JPT, Sept. 1980, pp 1509-1522.

23. G. P. Willhite, "Overall Heat Transfer Coefficients in Steam and Hot Water Injection Wells," JPT, Jan. 1967, pp. 607-615.

24. C. S. Holmes and S. C. Swift, "Calculation of Circulating Mud Temperatures," JPT, June 1970, pp 670-674.

25. L. R. Raymond, "Temperature Distribution in a Circulating Drilling Fluid," JPT, March 1969, pp 333-341.

References (cont)

26. D. D. Cline, "A Thermal Analysis of Pseudo-Steady Circulating Wellbores," Sandia National Laboratories, SAND81-0241, March 1981.

27. F. Kreith and W. Z. Black, Basic Heat Transfer, Harper and Row, New York, 1980.

28. A. M. Jessop, "Heat Flow in a System of Cylindrical Symmetry," Cdn. J. of Physics, Vol. 44, pp 677-679, 1966.

29. H. S. Carslaw and J. C. Jaeger, Conduction of Heat in Solids, Oxford University Press, New York, 1959.

30. D. E. Amos, "Heat Transfer into the Infinite Region External to a Cylinder," Sandia Laboratories, SAND78-1942, Nov. 1978.

WELLBORE SCHEMATIC

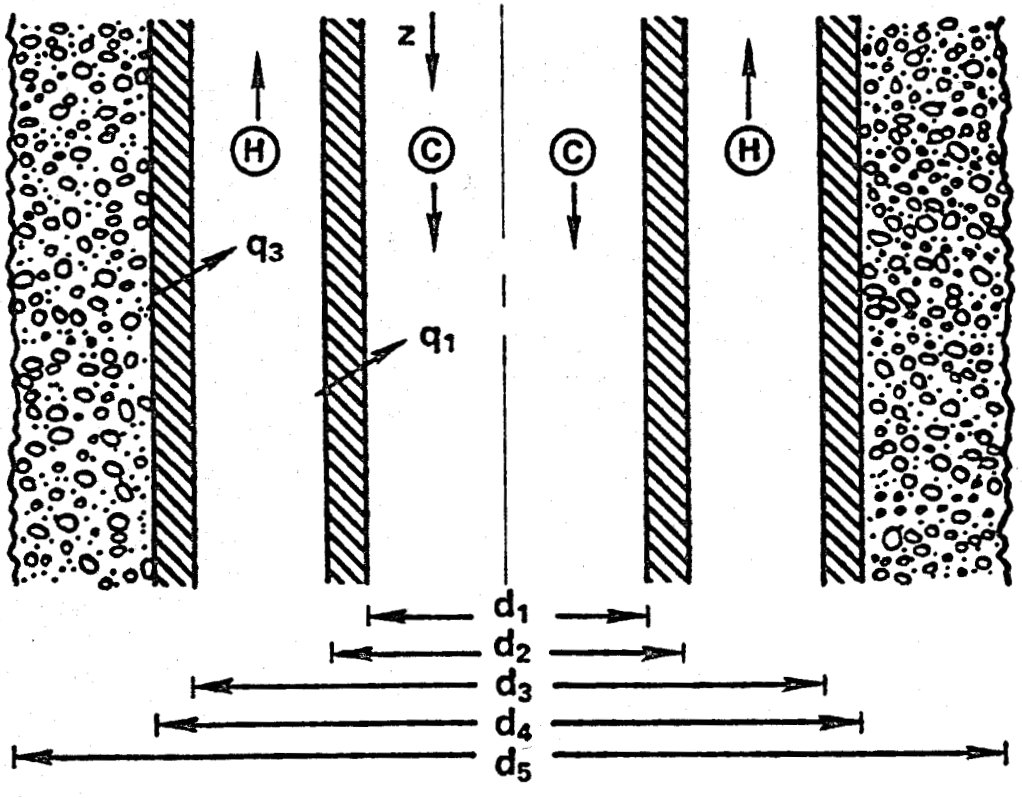

$$q_1 = U_1 (T_H - T_C)$$

$$q_3 = U_3 \left[T_\infty(z) - T_H \right]$$

FIGURE 1 SCHEMATIC OF SIMPLIFIED WELLBORE

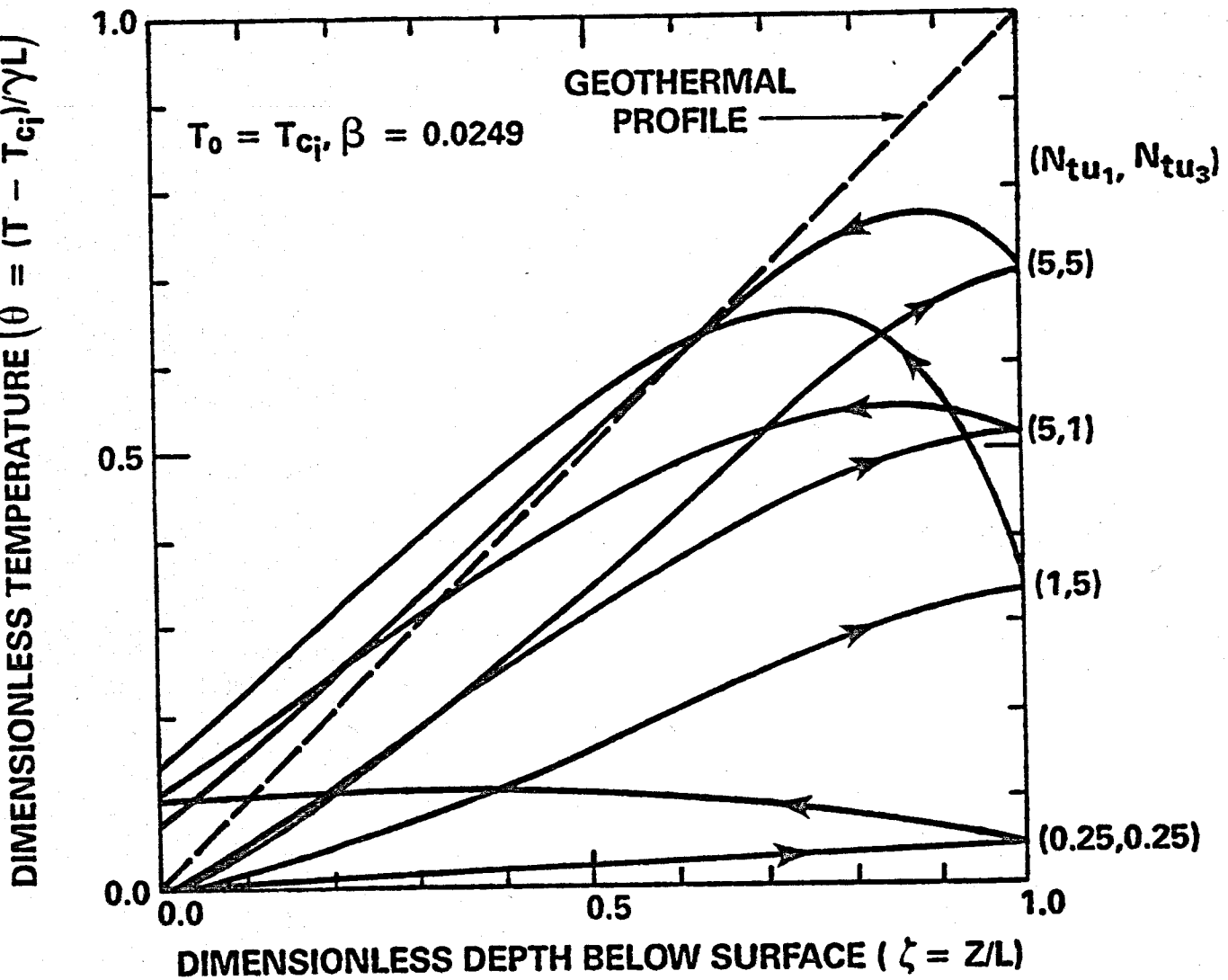

FIGURE 2 DIMENSIONLESS TEMPERATURE PROFILE FOR VARIOUS VALUES OF N_{tu_1} AND N_{tu_3}

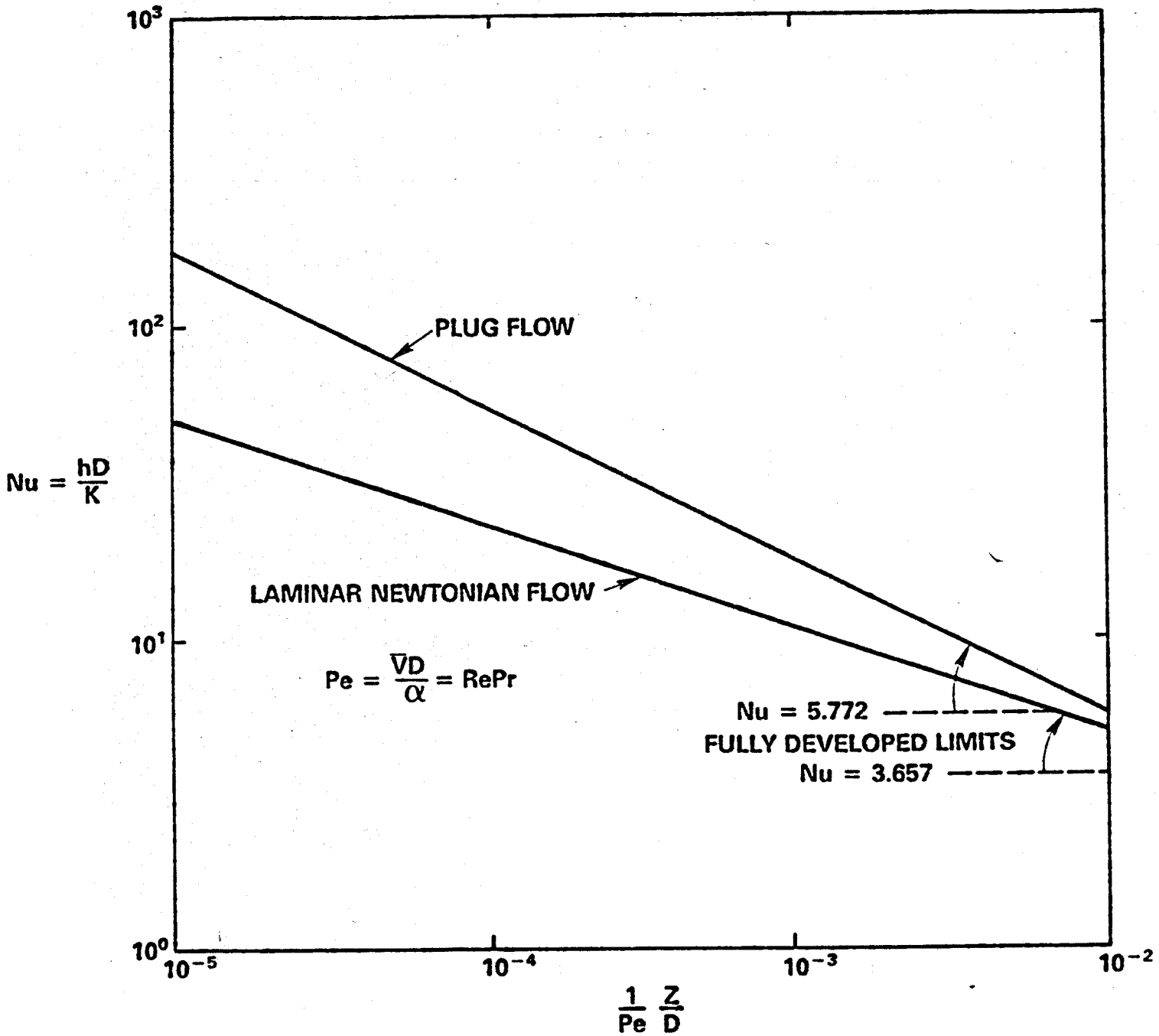

FIGURE 3 COMPARISON OF Nu VS Pe RELATIONSHIPS FOR LAMINAR NEWTONIAN AND PLUG FLOW IN A PIPE

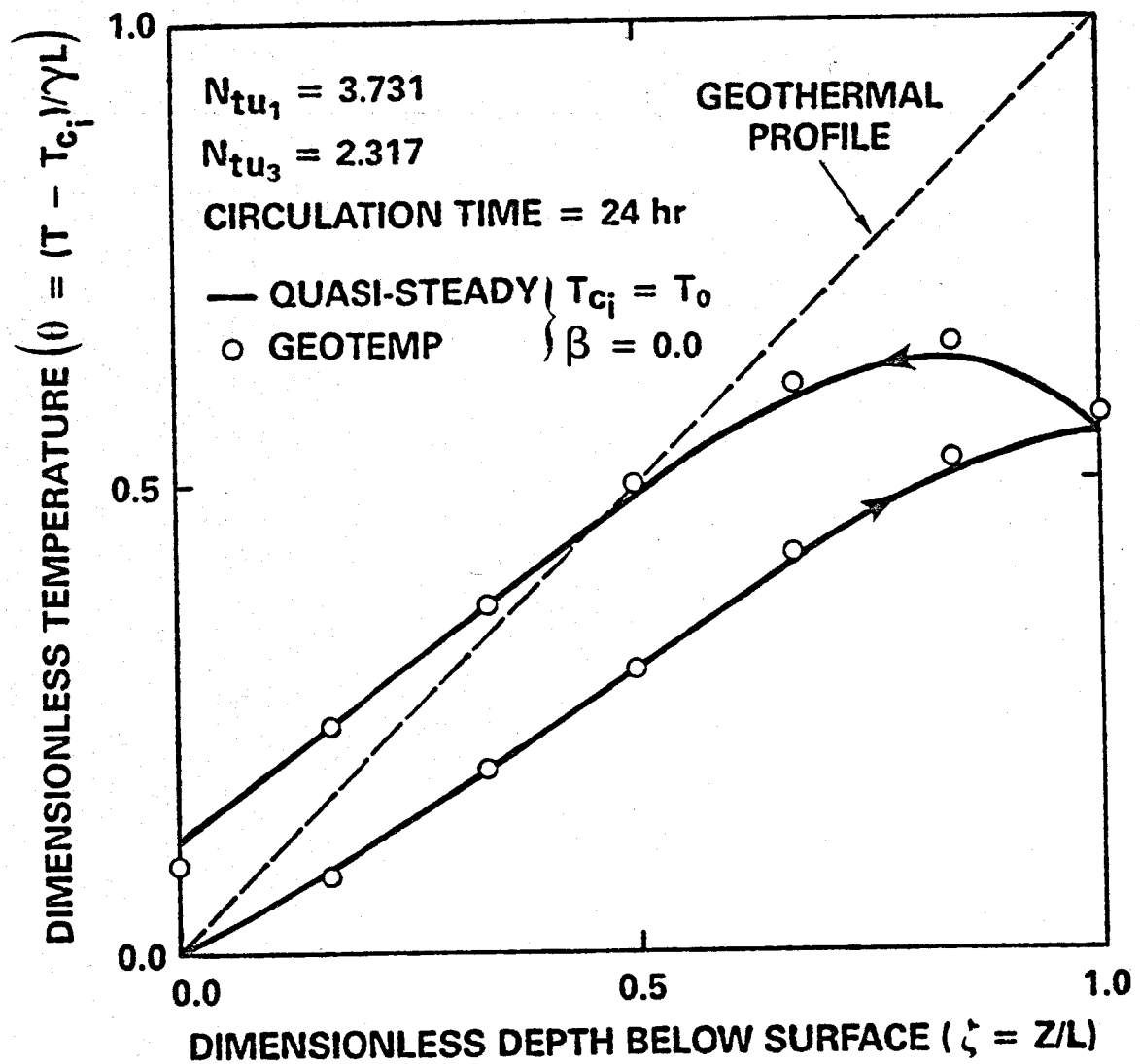

FIGURE 4 COMPARISON OF QUASI-STEADY MODEL WITH GEOTEMP CODE OF WOOLEY [20-22]

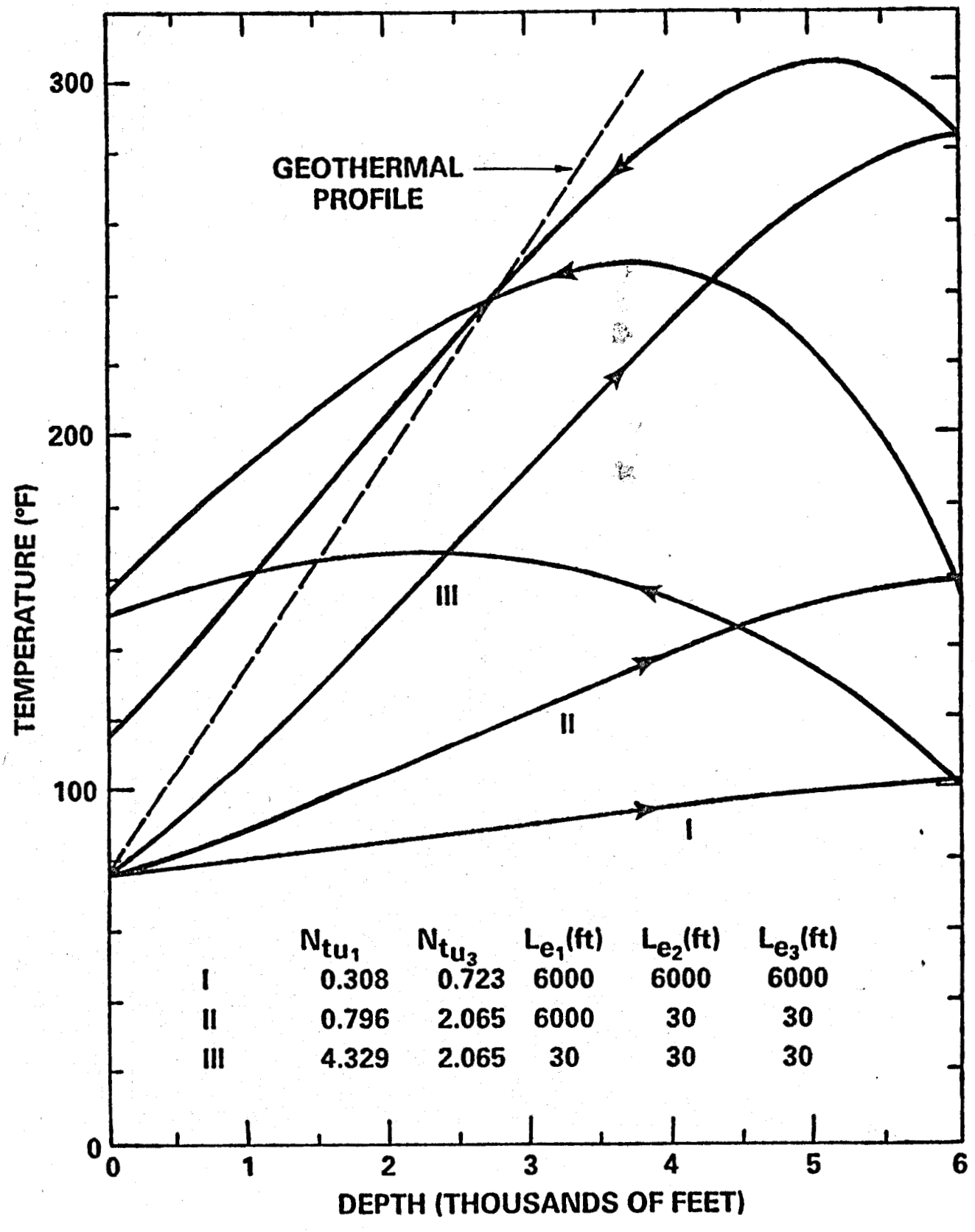

	N_{tu_1}	N_{tu_3}	L_{e_1}(ft)	L_{e_2}(ft)	L_{e_3}(ft)
I	0.308	0.723	6000	6000	6000
II	0.796	2.065	6000	30	30
III	4.329	2.065	30	30	30

FIGURE 5 COMPARISON OF TEMPERATURE PROFILES FOR DIFFERENT AVERAGING LENGTHS, PLUG FLOW

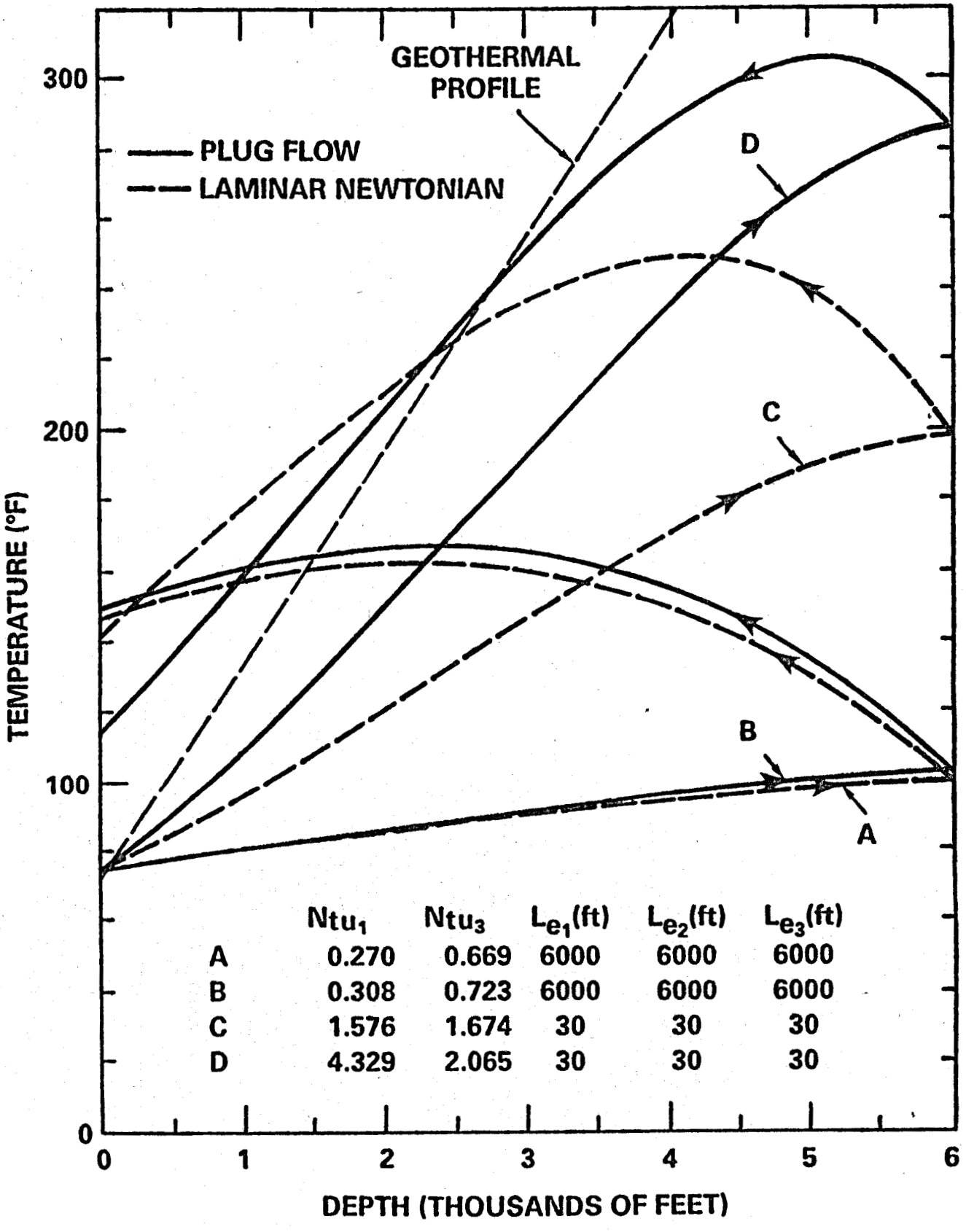

	Ntu_1	Ntu_3	L_{e_1}(ft)	L_{e_2}(ft)	L_{e_3}(ft)
A	0.270	0.669	6000	6000	6000
B	0.308	0.723	6000	6000	6000
C	1.576	1.674	30	30	30
D	4.329	2.065	30	30	30

FIGURE 6 COMPARISON OF PLUG FLOW AND LAMINAR NEWTONIAN FLOW HEAT TRANSFER MODELS

APPENDIX A

Detailed Development of Temperature Profile Model

The analysis that follows relies on earlier developments of Willhite [23], Holmes and Swift [24], Raymond [25], and Cline [26]. The primary difference between this development and that of Cline [26] is the inclusion of gravitational potential energy in the energy equation. Although some portions of this development can be found in some of the earlier works cited above, the details are repeated here for the sake of clarity and completeness.

Figure 1 presents a schematic of a simplified wellbore. Drill pipe of inside diameter d_1 is surrounded by casing of inside diameter d_3 and a cement liner of inside diameter d_4. This wellbore is obviously a simplification since it shows all diameters to be independent of depth. For the purpose of analysis, the fluid flowing down the drill pipe is designated the "cold" fluid while that flowing up the annulus is designated the "hot" fluid. The "cold" and "hot" fluids have the same temperature at the bottom of the wellbore provided one ignores the energy input into the drilling fluid by the drill bit. Heat is transferred from the formation to the hot fluid according to the following relation:

$$q_3(z,t) = U_3(t)[T_\infty(z)-T_h(z,t)] \tag{A-1}$$

where $T_\infty(z)$ is the undisturbed formation temperature far removed from the wellbore and is independent of time. $U_3(t)$ is the overall heat transfer coefficient between the undisturbed formation and the hot fluids; the procedures for calculating $U_3(t)$ are discussed in Appendix B.

Heat is assumed to be transferred from the "hot" fluid to the "cold" fluid by the following relationship:

$$q_1(z,t) = U_1[T_h(z,t)-T_c(z,t)] \tag{A-2}$$

The overall heat transfer coefficient U_1 is assumed to be independent of time and depth.

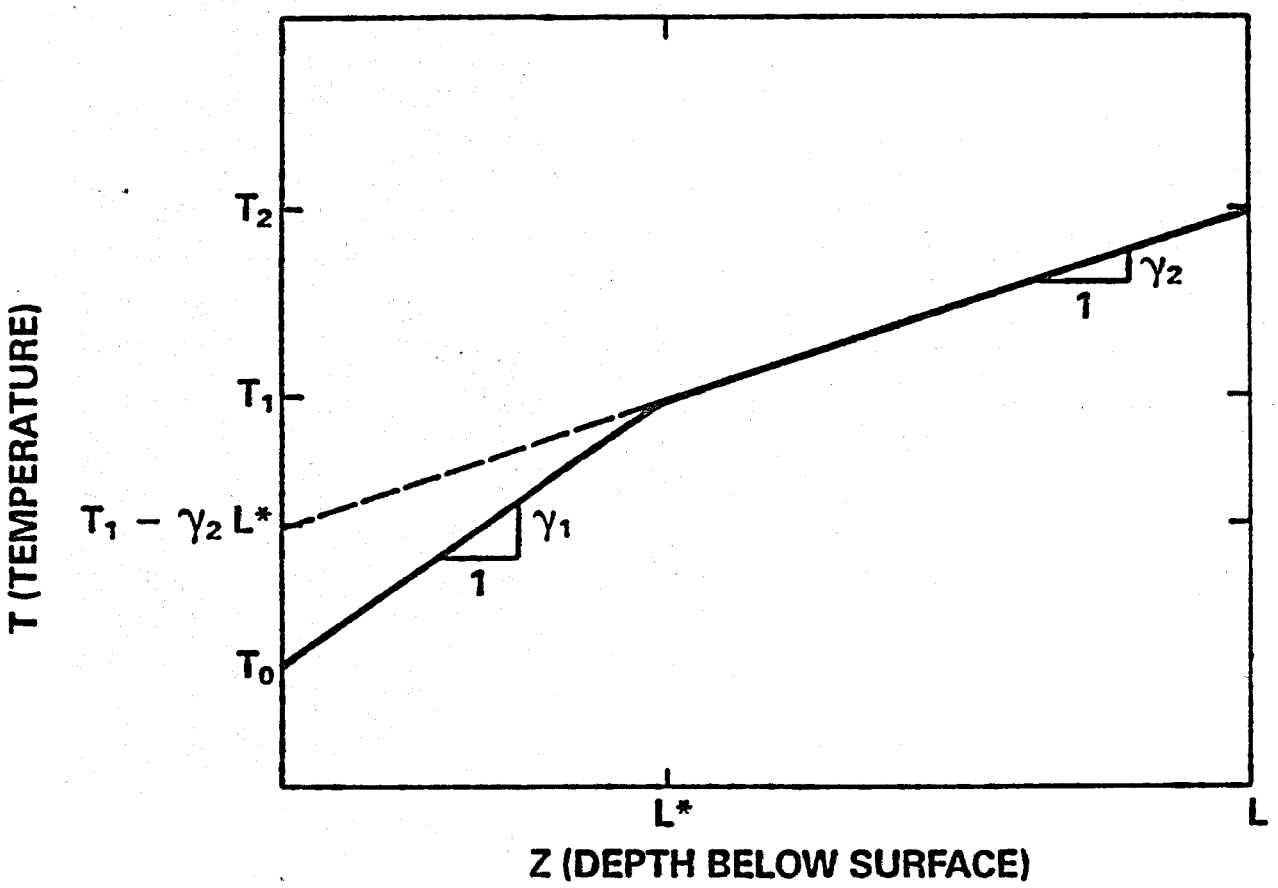

FIGURE A-1 SKETCH OF BI-LINEAR GEOTHERMAL PROFILE

An energy balance on the "cold" and "hot" fluids produces a pair of coupled first order ordinary differential equations:

$$\dot{m}\frac{d}{dz}\left(i_c - \frac{g}{g_c}\frac{z}{J}\right) - U_1 P_1 (T_h - T_c) = 0 \qquad \text{(A-3)}$$

$$-\dot{m}\frac{d}{dz}\left(i_h - \frac{g}{g_c}\frac{z}{J}\right) + U_1 P_1 (T_h - T_c) - U_3 P_3 [T_\infty(z) - T_h] = 0 \qquad \text{(A-4)}$$

Eqs. (A-3) and (A-4) are valid for steady one-dimensional flow of an incompressible fluid in which the kinetic energy is small in comparison to the enthalpy (i) and potential energy ($\frac{g}{g_c}\frac{z}{J}$). The term quasi-steady will be used to describe this model because the steady state form of the wellbore energy equation is used in conjunction with the transient heat transfer from the formation to the "hot" fluid. Although drilling foams are certainly compressible, the incompressible assumption allows the energy equation to be solved independent of the momentum equation, and should be valid for estimating the maximum foam temperature. The boundary conditions for Eqs (A-3) and (A-4) are

$$\left.\begin{aligned} T_c &= T_{c_i} \quad \text{at} \quad z=0 \\ T_h &= T_c \quad \text{at} \quad z=L \end{aligned}\right\} \qquad \text{(A-5)}$$

Replacing the enthalpy by heat capacity times temperature, the two energy balance equations can be combined to yield the following dimensionless equations:

$$-\frac{d^2\Theta_c}{d\zeta^2} + N_{tu_3}\frac{d\Theta_c}{d\zeta} + N_{tu_1}N_{tu_3}\Theta_c = N_{tu_1}N_{tu_3}\Theta_\infty(\zeta) + N_{tu_3}\beta \qquad \text{(A-6)}$$

where

$$\Theta_c = \frac{T_c - T_{c_i}}{\Delta T}, \quad \Delta T = T_2 - T_o, \quad \beta = \frac{gL}{g_c J c_p \Delta T}$$

$$\Theta_\infty(\zeta) = \frac{T_\infty(z) - T_{c_i}}{\Delta T}, \quad \zeta = z/L, \quad N_{tu_i} = \frac{(UA)_i}{\dot{m}c_p} \qquad \text{(A-7)}$$

with boundary conditions of the form

$$\theta_c = 0 \text{ at } \zeta=0$$
$$\frac{d\theta_c}{d\zeta} = \beta \text{ at } \zeta=1 \qquad \text{(A-8)}$$

Utilizing Laplace transforms, the solution to Eq. (A-6) can be written as

$$\theta_c(\zeta) = \frac{\theta_c'(0)}{\lambda_1-\lambda_2}(e^{\lambda_1\zeta}-e^{\lambda_2\zeta}) + \beta N_{tu_3}\left[\frac{1}{(\lambda_1-\lambda_2)}\left(\frac{e^{\lambda_1\zeta}}{\lambda_1} - \frac{e^{\lambda_2\zeta}}{\lambda_2}\right) + \frac{1}{\lambda_1\lambda_2}\right]$$
$$+ \frac{N_{tu_1}N_{tu_3}}{\lambda_1-\lambda_2}\int_0^{\zeta}(e^{\lambda_1\tau} - e^{\lambda_2\tau})\theta_\infty(\zeta-\tau)d\tau \qquad \text{(A-9)}$$

where

$$\lambda_1 = \frac{N_{tu_3}}{2}\left(1 + \sqrt{1+4\frac{N_{tu_1}}{N_{tu_3}}}\right),$$
$$\lambda_2 = \frac{N_{tu_3}}{2}\left(1 - \sqrt{1+4\frac{N_{tu_1}}{N_{tu_3}}}\right) \qquad \text{(A-10)}$$

The effects of gravity are contained in the term multiplied by β. The physical significance of β can be understood by grouping the term into two parts. The grouping $gL/(g_cJ)$ represents the potential energy change of a unit mass of fluid in moving from the top to bottom of the wellbore; the grouping $C_p\Delta T$ represents the enthalpy increase in changing a unit mass of drilling fluid from T_o to T_2 ($=T_o+\Delta T$), the undisturbed bottom hole formation temperature. Gravitational effects will certainly be negligible when $\beta<<1$.

Cline [26] has evaluated a term similar to the integral term in Eq. (A-9) for a geothermal temperature profile composed of two linear segments (bi-linear). Due to the complexity of the algebra of the Cline [26] result, an alternate approach was adopted. For the case of a bi-linear geothermal profile as shown in Figure A-1, the solution will be divided into two domains; within each domain the goethermal profile is as follows:

$$T_\infty(z) = T_o + \gamma_1 z, \quad 0 \le z \le L^*$$

$$T_\infty(z) = T_o + \gamma_1 L^* + \gamma_2 (z - L^*), \quad L^* \le z \le L$$

The corresponding dimensionless geothermal profile is

$$\theta_\infty(\zeta) = \frac{T_\infty(\zeta) - T_{c_i}}{T_2 - T_o} = \begin{cases} \dfrac{T_o - T_{c_i}}{\Delta T} + \dfrac{\gamma_1 L}{\Delta T}\,\zeta\,, & 0 \le \zeta \le \zeta^* \\ \dfrac{T_o - T_{c_i}}{\Delta T} + \dfrac{(\gamma_1 - \gamma_2)}{\Delta T}\,\zeta^* L + \dfrac{\gamma_2 L}{\Delta T}\,\zeta, & \zeta^* \le \zeta \le 1 \end{cases} \tag{A-12}$$

Eq. (A-6) can be applied over each of the two ranges, with $\theta_\infty(\zeta)$ given by Eq. (A-12). The appropriate boundary conditions are given by Eq. (A-8) along with the requirement that $\theta(\zeta^*)$ and $d\theta(\zeta^*)/d\zeta$ are continuous across the interface between the two regions. After some lengthy, but straight forward algebra, the solution for the temperature profile can be written as

$$\theta_c = \frac{T_c - T_{c_i}}{\Delta T} = \begin{cases} B_1\zeta + C_1 + D_1 e^{\lambda_1 \zeta} + E_1 e^{\lambda_2 \zeta}, & 0 \le \zeta \le \zeta^* \\ B_2\zeta + C_2 + D_2 e^{\lambda_2 \zeta} + E_2 e^{\lambda_2 \zeta}, & \zeta^* \le \zeta \le 1 \end{cases} \tag{A-13}$$

where the above constants are defined as follows:

$$B_1 = \frac{\gamma_1 L}{\Delta T}\,, \quad C_1 = \frac{T_o - T_{c_i}}{\Delta T} + \frac{1}{N_{tu_1}}\left(\beta - \frac{\gamma_1 L}{\Delta T}\right)$$

$$B_2 = \frac{\gamma_2 L}{\Delta T}\,, \quad C_2 = \frac{T_o - T_{c_i}}{\Delta T} + \frac{(\gamma_1 - \gamma_2)}{\Delta T}\zeta^* L + \frac{1}{N_{tu_1}}\left(\beta - \frac{\gamma_2 L}{\Delta T}\right)$$

$$H = \left(1 - \frac{\lambda_2}{\lambda_1}\right) \frac{e^{\lambda_1(\zeta^*-1)}\, e^{\lambda_2(\zeta^*-1)}}{e^{\lambda_2(\zeta^*-1)} - \dfrac{\lambda_2}{\lambda_1} e^{\lambda_1(\zeta^*-1)}} \left(\lambda_2 e^{\lambda_2} - \lambda_1 e^{\lambda_1}\right) \tag{A-14}$$

$$P = \frac{\lambda_2 \left(e^{\lambda_2(\zeta^*-1)} - e^{\lambda_1(\zeta^*-1)}\right)}{e^{\lambda_2(\zeta^*-1)} - \dfrac{\lambda_2}{\lambda_1} e^{\lambda_1(\zeta^*-1)}}$$

$$E_1 = \frac{C_1 e^{\lambda_1 \zeta^*}(\lambda_1 - P) + (B_2 - B_1)(1 - P\zeta^*) - P(C_2 - C_1) + (\beta - B_2)e^{\lambda_1(\zeta^* - 1)}(1 - \frac{P}{\lambda_1})}{\Pi}$$

$$E_2 = \frac{E_1(e^{\lambda_2 \zeta^*} - e^{\lambda_1 \zeta^*}) - C_1 e^{\lambda_1 \zeta^*} - (B_2 - B_1)\zeta^* - (C_2 - C_1) - \frac{(\beta - B_2)}{\lambda_1} e^{\lambda_1(\zeta^* - 1)}}{e^{\lambda_2}(e^{\lambda_2(\zeta^* - 1)} - \frac{\lambda_2}{\lambda_1} e^{\lambda_1(\zeta^* - 1)})}$$

$$D_1 = -(C_1 + E_1) \quad , \quad D_2 = \frac{\beta - B_2 - \lambda_2 E_2 e^{\lambda_2}}{\lambda_1 e^{\lambda_1}}$$

Once the "cold" fluid temperature profile is known, the "hot" fluid temperature profile can be computed from the "cold" fluid energy balance.

$$\theta_h = \theta_c + \frac{1}{N_{tu_1}} (\frac{d\theta_c}{d\zeta} - \beta) \qquad \text{(A-15)}$$

$$\theta_h = \begin{cases} B_1(\zeta + \frac{i}{N_{tu_1}}) + C_1 - \frac{\beta}{N_{tu_1}} + (1 + \frac{\lambda_1}{N_{tu_1}})D_1 e^{\lambda_1 \zeta} + (1 + \frac{\lambda_2}{N_{tu_1}})E_1 e^{\lambda_2 \zeta}, & 0 \le \zeta \le \zeta^* \\ B_2(\zeta + \frac{1}{N_{tu_1}}) + C_2 - \frac{\beta}{N_{tu_1}} + (1 + \frac{\lambda_1}{N_{tu_1}})D_2 e^{\lambda_2 \zeta} + (1 + \frac{\lambda_2}{N_{tu_1}})E_2 e^{\lambda_2 \zeta}, & \zeta^* \le \zeta \le 1 \end{cases} \qquad \text{(A-16)}$$

From the solution presented above, one can identify six dimensionless parameters that are necessary to determine the dimensionless temperature profile (θ vs ζ):

$\beta = \frac{gL}{g_c J c_p \Delta T}$: gravitational

$\frac{T_o - T_{c_i}}{\Delta T}$: formation to cold fluid temperature difference at surface

$\zeta^* = \frac{L^*}{L}$: fractional depth at which two linear geothermal profiles are joined

$\frac{\gamma_1 L^*}{\Delta T} = \frac{\gamma_1 \zeta^*}{\gamma_1 \zeta^* + \gamma_2(1 - \zeta^*)}$: fractional formation temperature increase over first linear segment

$$N_{tu_1} = \frac{U_1 A_1}{\dot{m} C_p} \quad : \quad \text{number of transfer units}$$

$$N_{tu_3} = \frac{U_3 A_3}{\dot{m} C_p} \quad : \quad \text{number of transfer units}$$

The gravitational parameter β always appears either as $(\beta - B_1)$ or $(\beta - B_2)$. The effects of gravity can be safely ignored when

$$\frac{gL}{g_c J C_p \Delta T} << \frac{\gamma_{1,2} L}{\Delta T}$$

or,

$$\frac{g}{g_c J C_p \gamma_{1,2}} << 1 \quad \text{(gravity negligible)} \qquad \text{(A-17)}$$

Note that Eq. (A-17) is independent of the wellbore depth L; this condition can be satisfied by drilling fluids with large values of C_p and/or $\gamma_{1,2}$. Eq. (A-17) is conservative because even if it is violated, gravitational effects are not necessarily significant.

The grouping $N_{tu} = UA/\dot{m}C_p$ is given the name Number of Transfer Units. This name comes from the heat exchanger literature; drilling fluid circulating through a wellbore is similar to a counter flow heat exchanger with both fluids being the same. Physically, N_{tu} represents the bulk fluid temperature rise normalized by the heat transfer driving potential. High drilling fluid temperatures will result from large values of N_{tu}. Large values of N_{tu} occur when the overall heat transfer rates (U_1 and U_3) are large, heat transfer areas (A_1 and A_3) are large, and the capacity rate $\dot{m}C_p$ is small.

Note that the bi-linear solution given above reduces to the linear case when $\zeta^* = 1$. For this condition, P in Eq. (A-14) becomes identically zero. Only the constants (B_1, C_1, D_1, E_1) are necessary for the linear case and the equations defining them become simpler than Eq. (A-14). This result was presented in the text as Eqs. (3-5).

*The notation $\gamma_{1,2}$ means either γ_1 or γ_2.

APPENDIX B

Determination of Overall Heat Transfer Coefficients

Following the procedures outlined in introductory heat transfer texts (e.g. Kreith and Black [27]) or the more specific results of Willhite [23] for wellbores, one can write the overall heat transfer coefficient U_1 as

$$U_1 A_1 = \frac{\pi d_1 L}{\frac{1}{\bar{h}_1} + \frac{d_1}{2k_p} \ln(d_2/d_1) + \frac{d_1}{d_2}\frac{1}{\bar{h}_2}} \qquad \text{(B-1)}$$

where $\bar{h}_1$ and $\bar{h}_2$ are the average convective heat transfer coefficients on the inside and outside surfaces of the drill pipe respectively and k_p is the thermal conductivity of the pipe. The wellbore geometry is defined in Figure 1. For many applications, the thermal resistance of the pipe wall can be ignored; it is included here for the sake of completeness.

The transient heat transfer by conduction within the formation is assumed to be one dimensional radial heat transfer in an infinite medium. Following procedures similar to those of Jessop [28] and Willhite [23], the overall heat transfer coefficient U_3 for heat transfer from the formation to the hot fluid can be written as

$$U_3 A_3 = U_3^o A_3 G(Fo, Bi) \qquad \text{(B-2)}$$

where U_3^o is the value of U_3 at time zero when $T_5 = T_\infty(z)$; U_3^o can be calculated from

$$U_3^o A_3 = \frac{\pi d_5 L}{\frac{d_5}{d_3}\frac{1}{\bar{h}_3} + \frac{d_5}{2k_p} \ln(d_4/d_3) + \frac{d_5}{2k_c} \ln(d_5/d_4)} \qquad \text{(B-3)}$$

with k_c being the thermal conductivity of the cement. The Fourier and Biot modulii for the wellbore are given by

$$Fo = \frac{4\alpha_e t}{d_5^2} \quad , \quad Bi = \frac{U_3^o d_5}{2k_e} \tag{B-4}$$

with α_e and k_e being the thermal diffusivity and thermal conductivity of the formation (earth) respectively. The function G(Fo,Bi) can be computed from an anlytical solution in Carslaw and Jaeger [29] for the response of an infinite region bounded internally by a hole of radius $r_5 = d_5/2$ and subjected to a convective boundary condition of the form

$$-k_e \left.\frac{\partial T}{\partial r}\right|_{r=r_5} = U_3^o[T_h - T(r_5,t)] \tag{B-5}$$

The result for G(Bi,Fo) is

$$G(Fo,Bi) = \frac{1}{Bi}\left(\frac{2}{\pi}\right)^2 \int_0^\infty \frac{\exp(-Fox^2)}{\left[\frac{x}{Bi} J_1(x)+J_0(x)\right]^2+\left[\frac{x}{Bi} Y_1(x)+Y_0(x)\right]^2} \frac{dx}{x} \tag{B-6}$$

where J_0, J_1, Y_0 and Y_1 are Bessel functions of the 1st and 2nd kind respectively of order 0 and 1. The general computer routine developed by Amos [30] for evaluating Eq. (B-6) was used for all of the numerical results of this study. Table B-1 presents a summary of some of the results from Eq. (B-6). Note that G(0,Bi) is unity for all values of Bi, and for a given value of Bi, G(Bi,Fo) is a monatonically decreasing function of Fo. Additional values of integrals related to G(Fo,Bi) are tabulated in Willhite [23] and Jessop [28]. For example, the function f given by Willhite [23] is related to G(Bi,Fo) by

$$G = \frac{1}{1+fBi} \tag{B-7}$$

If the integral tabulated by Jessop [28] is denoted by I_J, then

$$G = \left(\frac{2}{\pi}\right)^2 \frac{1}{Bi} I_J \tag{B-8}$$

The definition of G(Bi, Fo) used in this study was chosen primarily because it is bounded by the range $0 \leq G \leq 1$.

The above approach to calculating the heat loss from the formation assumes that heat transfer through the cement and casing is steady state while that in the formation is transient

Table B-1: Tabulation of the function G(Bi,Fo) using the method of Amos [30]

	G(Bi,Fo)				
Fo\Bi	0.01	0.1	1.0	10.0	100.0
0.0	1.0	1.0	1.0	1.0	1.0
0.1	0.99687	0.96936	0.75132	0.20098	0.02230
1.0	0.99203	0.92496	0.53429	0.09226	0.00978
10.0	0.98374	0.85662	0.36055	0.05109	0.00532
100.0	0.97346	0.78411	0.26032	0.03348	0.00344
1000.0	0.96279	0.71988	0.20177	0.02450	0.00250
10000.0	0.95225	0.66495	0.16430	0.01922	0.00196

Distribution:

TID-4500-R66-UC-66c (507)

Tom Anderson
Venture Innovations
P.O. Box 35845
Houston, Texas 77035

Ed Bingman
Shell Oil Company
Two Shell Plaza
P.O. Box 2099
Houston, Texas 77001

Larry Diamond
Dyna-Drill
P.O. Box C-19576
Irvine, California 92713

John E. Fontenot
NL Petroleum Services
P.O. Box 60087
Houston, Texas 77205

Dr. Melvin Friedman
Professor of Geology
Center for Tectonophysics
and Dept. of Geology
Texas A&M University
College Station, Texas 77843

Tom Turner
Phillips Petroleum Company
Geothermal Operations
655 East 4500 South
Salt Lake City, Utah 84107

Jim Kingsolver
Geothermal Operations
Smith Tool
P.O. Box C-19511
Irvine, California 92713

James W. Langford
Security Division
Dresser Industries, Inc.
P.O. Box 24647
Dallas, Texas 75224

Harvey E. Mallory
P.O. Box 54696
Tulsa, Oklahoma 74155

Gene Polk
NL Baroid
6400 Uptown Blvd. N.E. 365W
Albuquerque, New Mexico 87110

Del E. Pyle
Union Geothermal Division
Union Oil Co. of California
Union Oil Center
Los Angeles, California 90017

John C. Rowley
Los Alamos Nat'l Scientific Lab.
Mail Stop 570
Los Alamos, New Mexico 87545

William D. Rumbaugh
Research and Development
Otis
P.O. Box 34380
Dallas, Texas 75234

Dwight Smith
Halliburton
Drawer 1431
Duncan, Oklahoma 73533

Tom Warren
Amoco Production Company
Research Center
P.O. Box 591
Tulsa, Oklahoma 74102

Distribution (cont)

Ed Martin
Superior Oil
Eastern Division
P.O. Box 51108 OCS
Lafayette, Louisiana 70505

B. J. Livesay
129 Liverpool
Cardiff, California 92007

U.S. Department of Energy (4)
Geothermal Hydropower
Technologies Division
Forrestal Bldg., CE 324
1000 Independence Aven. S.W.
Washington, D.C. 20585
Attn: J. Bresee
D. Clements
R. Toms
D. Allen

W. P. Grace, DOE/ALO
Nuclear & Geosciences Division

1500 W. Herrmann
1510 D. B. Hayes
1511 C. E. Hickox
1512 D. F. McVey (2)
1512 L. A. Mondy
1513 D. D. Cline
1813 A. M. Kraynik
1813 P. B. Rand
1824 W. D. Drotning
3141 L. J. Erickson (5)
3151 W. L. Garner (3)
7530 W. E. Caldes
attn: N. R. Keltner (7537)
7537 B. F. Blackwell (10)
9000 G. A. Fowler
9700 E. H. Beckner
9740 R. K. Traeger
9741 J. R. Kelsey (10)
9741 C. C. Carson
9743 H. C. Hardee
9746 B. Granoff
9747 P. J. Hommert
9750 V. L. Dugan
9760 R. W. Lynch
9770 G. E. Brandvold
8214 M. A. Pound